

Solution Synthesis of Germanium Nanocrystals: Success and Open Challenges

Daniele Gerion,^{*,†} Natalia Zaitseva,[†] Cheng Saw,[‡] Maria Francesca Casula,[§] Sirine Fakra,^{||} Tony Van Buuren,[‡] and Giulia Galli[†]

Physics and Advanced Technology, Lawrence Livermore National Laboratory, Livermore, California 94551, Chemistry and Materials Sciences, Lawrence Livermore National Laboratory, Livermore, California 94551, Dipartimento di Scienze Chimiche, Universita di Cagliari, Italy, and Advanced Light Source, Lawrence Berkeley National Laboratory, Berkeley, California 94720

Received December 23, 2003; Revised Manuscript Received February 5, 2004

ABSTRACT

We present a two-step synthesis route that yields nanometer-size crystalline germanium in the form of a black powder. It relies on high temperature decomposition of tetraethylgermane (TEG) in organic solvents. The presence of pure germanium with diamond structure is unambiguously attested by powder XRD measurements. Low-resolution TEM indicates that the particles are between ~5 to 30 nm in size, depending on the synthesis conditions. The as-synthesized Ge powders can be stored in air for months and no oxidation occurs. The Ge powders are sparingly soluble in conventional solvents because Ge nanocrystals are likely embedded in a matrix composed mainly of C=C, C–C, and C–H bonds. The presence of residual organic byproducts impedes probing of the optical properties of the dots. Also, we discuss drawbacks and open challenges in high-temperature solution synthesis of Ge nanocrystals that could also be faced in the synthesis of Si nanocrystals. Overall, our results call for a cautious interpretation of reported optical properties of Ge and Si nanocrystals obtained by high-temperature solution methods.

The suggestion that nanometer-size silicon and germanium crystals may have a strong photoluminescence has generated a great deal of excitement because in the bulk both materials emit light poorly. It has been proposed that below a certain critical size of a few nanometers, optical band gap transitions change from indirect to direct, due to the breaking of translational symmetry.¹ A direct optical band gap reduces markedly the lifetime of the excitons, since phonons would not be involved in the recombination process. This has profound implications for optoelectronic applications, since nanocrystals of Si and Ge capable of direct band gap transitions could act as efficient electronic devices² and light emitters.³

A large number of different methods of synthesis of Si and Ge nanocrystals have been reported including etching,⁴ MBE,⁵ PECVD,⁶ ion implantation,⁷ and gas evaporation.⁸ However, they all yield microscopic amounts of material that are often complex to characterize and almost impossible to process. Our goal is to synthesize macroscopic amounts of

Si and Ge nanocrystals in a simple and robust way, which allows a full characterization of the nanocrystals and permits their subsequent processing and integration into working devices. Solution synthesis of free-standing colloidal nanocrystals seems a promising route. Some solution syntheses have been reported at low^{9–12} or high¹³ temperature by reducing silicon or germanium tetrachloride. These approaches rely on complex reaction mechanisms and often yield a significant amount of byproducts that are difficult to remove. A cleaner and apparently simpler approach is to thermally degrade precursors and supersaturate the solution with monomers of Ge and Si that would eventually nucleate. This approach requires high temperatures to decompose the Ge and Si precursors and avoid the formation of amorphous Si and Ge species.^{14,15} So far, however, high temperature solution syntheses provide only microscopic amounts of nanocrystals that can sparsely cover a TEM grid and cannot be characterized with established bulk techniques such as powder X-ray diffraction.

A general trend for the formation of crystalline nuclei of semiconductor elements is that the more covalent the element the higher its crystallization temperature.¹⁶ At low temperatures, amorphous phases become more common as the material becomes more covalent. Thus, if high quality ionic

* Corresponding author. E-mail: gerion1@llnl.gov. Tel: 925-423-2208.

† Physics and Advanced Technology, LLNL.

‡ Chemistry and Materials Sciences, LLNL.

§ Universita di Cagliari.

|| Advanced Light Source, LBNL.

II–VI semiconductors (i.e., CdSe) can be synthesized at moderate temperature, III–V nanocrystals (i.e., InP) require temperatures close to 250 °C for many days.¹⁷ Covalent IV nanocrystals (i.e., Si and Ge) are expected to require even higher temperatures, possibly above 400 °C. Solution syntheses at those high temperatures pose a serious challenge since most organic solvents, including pentane and longer alkyl chains, are unstable. They decompose into reactive free radicals and exhibit blue fluorescence. Therefore, the question of whether Ge and Si nanocrystals can be synthesized at high temperature from organogermane (or organosilane) precursors in organic solvents is far from trivial.

In this letter, we present a simple two-step synthesis that produces amounts of germanium nanocrystals that can be measured by X-ray diffraction and TEM. First a germanium precursor, tetraethylgermane (TEG), is decomposed at 430 °C in a high-pressure reactor generating on the order of 1 g of a black powder. This powder consists of Ge nanocrystals embedded in a matrix that is a byproduct of the reaction. In a second step, the matrix is dissolved and Ge nanocrystals are recovered. The dissolution step represents the most challenging step. Free colloidal Ge nanoparticles represent only a few percent of the black Ge powder, and thus large quantities of Ge nanocrystals are not yet available. However, the general concept of a two-step or multistep synthesis should be a viable route to make near-gram quantities of Ge dots, if control of the matrix dissolution can be achieved.

The synthesis is performed in a 250 mL Hastelloy Parr reactor (model 4576A, Parr Company, Moline, IL), equipped with a thermocontroller, a magnetic stirrer, a cooling coil, and a calibrated transducer to measure the pressure. The reactor is evacuated to a pressure of ~200 mTorr and flushed with Ar many times. A stock solution of germanium is sealed in a glovebox and then connected to the reactor where it is sucked in. Pressure in the reactor is increased to slightly above 1 atm with Ar. The vessel is heated to ~430 °C in about 45 min and kept at this temperature for a defined period of time ranging from 1 min to 30 min. The temperature inside the vessel is then lowered by circulating cold water through a coil inside the reactor. The temperature drops to ~300 °C within one minute and to <100 °C within 1 h. During the heat-up, at around 400–420 °C, an abrupt increase in pressure (up to a 3-fold increase) indicates that molecules of the stock solution undergo extensive decomposition. Therefore, when back at room temperature, there is a residual overpressure. The residual pressure is released and the reactor is opened in air. We use different types of stock solution: (1) pure TEG, from 3 mL to 30 mL, (i.e., from 16 to 160 mmol) and (2) a mixture of TEG dissolved in hexane or toluene in v/v ratios of 1:80 to 1:1 with a final volume from 25 mL to 80 mL. We choose TEG because extensive studies in the 1930s pinpointed precisely its decomposition temperature and its products of reaction.¹⁸ In particular, decomposition of TEG was reported to produce pure Ge in a high yield.

For each type of stock solution (pure TEG, TEG in solvents), a visual inspection of the vessel after reaction shows the presence of a fine black powder deposited on its interior surface. If only pure TEG is used (a liquid), there is

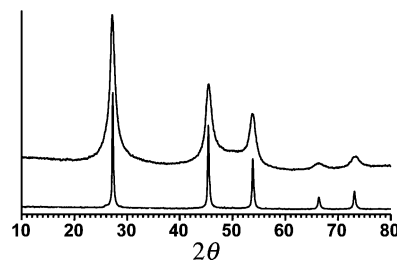


Figure 1. Examples of XRD spectra of as-synthesized black powders. The diffraction pattern corresponds to pure cubic Ge whose domain size is estimated to be ~6 nm (top) and >30 nm by the Scherrer formula. XRD analysis performed with Cu K_{α1} radiation (1.54056 Å) gives peak positions at $2\theta = 27.58, 45.67, 54.10, 66.46, \text{ and } 73.30^\circ$, close to the bulk values.

no, or trace amounts of, residual liquid left in the vessel. In contrast, if TEG is mixed with hexane or toluene there is a residual liquid (estimated from <50% to 80% of the initial injected volume) in addition to the black powder. The liquid is yellow and shows a strong blue-green luminescence under long wavelength illumination of a handheld UV lamp. This residual liquid is discarded since quick-scan TEM inspection indicates mainly the presence of amorphous organic compounds. The fine black powder can be removed easily from the vessel with a spatula and can be weighed. As a guideline, if we use 5 g of TEG precursors (equivalent to ~1.9 g of elemental Ge) we collect about 0.9 g of black powder.

Aliquots of these as-synthesized black powders are analyzed by powder X-ray diffraction (XRD, Figure 1). Black powders produced by the decomposition of TEG, with or without organic solvent (hexane and toluene), do exhibit the undisputably clear signature of pure diamond-phase germanium. The diffraction peaks in the XRD spectra show clear broadenings and have Lorentzian shapes. Such XRD patterns are compatible with the presence of either monocrystalline nanocrystals or polycrystalline bulk-like Ge. An estimation of the size of the Ge crystalline domains by the Debye–Scherrer formula indicates that average domain sizes vary from ~6 nm to ~30 nm, depending on the synthesis. The black powder is homogeneous since different aliquots show almost overlapping XRD patterns. We do not observe significant solvent-related differences in the XRD spectra of the powders. The presence of an organic solvent (hexane or toluene) does not produce a marked broadening or sharpening of the XRD patterns. The powders can be stored in air for months, with no modification of their XRD pattern. This observation suggests some sort of Ge–C shell around the Ge crystals that we will discuss later in the letter.

As shown in Figure 2, these as-synthesized powders were dispersed in different solvents and analyzed by TEM. The presence of Ge crystals with various dimensions (from ~7 nm up to 32 nm) is obvious. Sometimes we also observe the presence of amorphous byproducts. Germanium nanocrystals have various shapes: spheres, cubes, pyramids, and possibly rods and branched rods. These shapes are all compatible with the 3-dimensional symmetry of cubic Ge. In general, when we succeed in removing organic byproducts from the solution, Ge nanocrystals are observed to self-assemble on the TEM grid. The size distribution of the

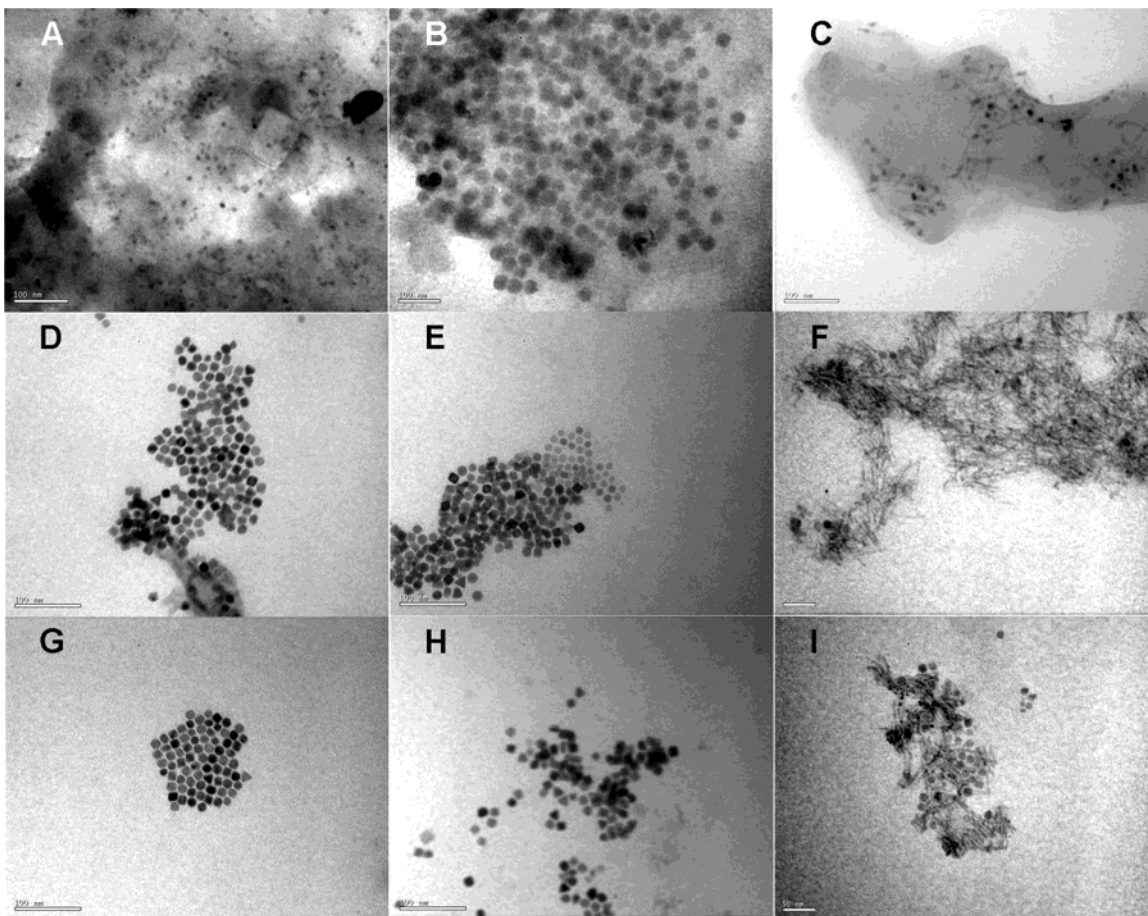


Figure 2. Composite figure of the various as-synthesized powders suspended in different solvents. Note the different shapes even within the same assemblies. A–C: Ge crystals in toluene. (A) 7.5 ± 2 nm Ge dots. (B) 32 ± 3.9 nm dots. (C) Branched Ge. D–G: Ge crystals in nonanoic acid. (D) 12.7 ± 1.2 nm Ge dots. (E) 11.7 ± 2 nm Ge dots. (F) Ge rods. (G) 12.7 ± 1.2 nm Ge dots. H–I: Ge crystals in methanol. (H) 15 ± 3 nm dots. (I) Dots and rods. Sizes and size distributions are determined by counting > 120 dots on representative TEM pictures of the samples. Bars: 100 nm, except 50 nm for F and I. The images were taken with a Tecnai 12 TEM at 100 kV and recorded with a digital camera. Images have not been processed. Additional TEM images are available in Supporting Information.

nanocrystals observed on TEM images determined by a statistical analysis of many images of the same batch reaction is ~ 10 – 20% . Additional TEM images are available in the Supporting Information. Whether such particle size is representative of the whole as-synthesized powder and why assemblies contain particles of roughly the same size are open questions.

We observe the presence of Ge nanocrystals for concentrations of TEG above a certain value, regardless of the volume of the stock solution and the presence of hexane or toluene in the stock solution. This minimal concentration of TEG is, however, not well characterized. As a guideline, when we use 3 g of TEG (~ 16 mmol) in 22 mL of hexane, we always synthesize pure Ge. In contrast, when we use 1 g (~ 5.3 mmol) of TEG in 24 mL of hexane, we are not guaranteed to obtain pure Ge. Indeed, for some of these syntheses at low TEG content, we do obtain a fine black powder that is visually indistinguishable from pure Ge. However, XRD analysis unambiguously reveals that this powder is not pure Ge, although it is crystalline, but with diffraction peaks at wide angles indicative of a small lattice spacing. Similarly, the presence of surfactants (octanol and octanethiol/TEG at a 1:3 molar ratio) does not markedly

affect the formation of Ge nanocrystals for TEG concentrations above ~ 25 mmol, although surfactants undergo extensive decomposition. The reason may well be that, at low TEG concentrations, side reactions of Ge monomers with impurities prevail. These impurities include reactive free radicals from TEG, or solvent and surfactant decomposition. Finally, Ge nanocrystals are obtained only above a certain temperature. For instance, if pure TEG is heated to 425 °C for 1 min we obtain Ge nanocrystals while if pure TEG is heated to 411 °C for 15 min, we do not observe any black powder although a sudden increase in pressure at ~ 400 °C indicates the onset of the TEG decomposition.

Although the XRD analysis indicates the presence of nanometer-size Ge crystals in the as-synthesized black powder, the synthesis is difficult to control. Similar runs always produce Ge nanocrystals but the width of the XRD peaks varies markedly from one run to the other. Estimated sizes from XRD spectra may range from ~ 6 nm to ~ 15 nm for syntheses performed under similar conditions. This low level of control prevents a thorough and systematic study of the effects of different parameters on the final average size of the nanocrystals. As a matter of fact, the as-synthesized black powders are easily resuspended in most solvents,

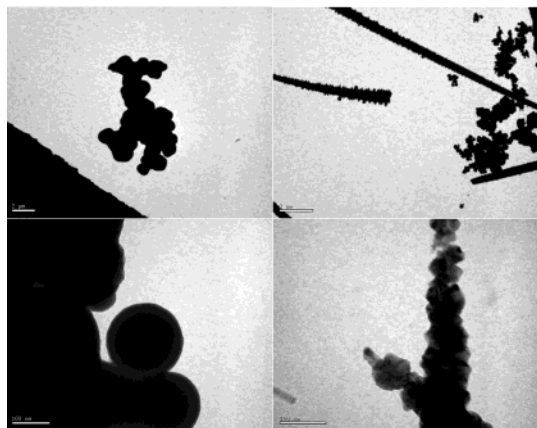


Figure 3. TEM views of as-synthesized powders that do not dissolve in toluene at various magnifications. Notice the different morphologies from purely spherical to elongated shapes. Both can be seen on the same TEM grid. Scale bars: 2 μm (top), 100 nm (bottom).

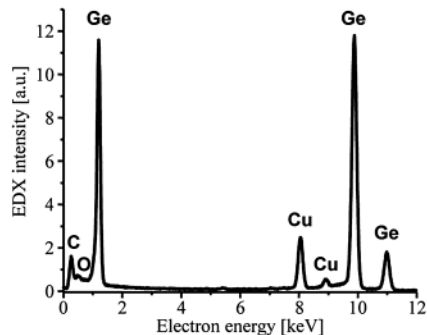
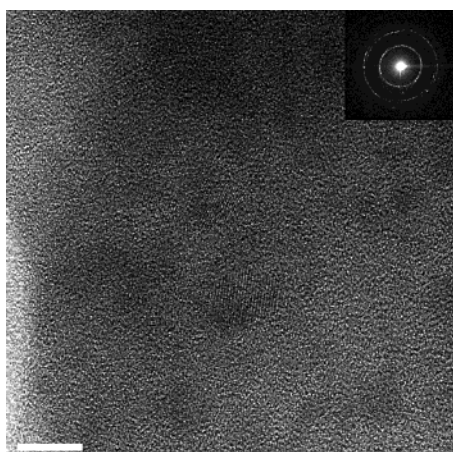


Figure 4. HRTEM and EDX analyses of the as-synthesized powders showing that (1) the powders show the presence of Ge crystalline particles embedded in a matrix as evidenced by electron diffraction (top, inset) and (2) they contain only Ge and C (Cu coming from the TEM grid). Scale bar: 10 nm.

although they are sparingly soluble in them. Figure 3 shows a few typical TEM images of suspensions of black powders in toluene at different magnifications. Note that Figure 2 and Figure 3 are both from black powder samples and Figure 3 represents the large majority of the powders. These have micron to submicron size features. They also possess various morphologies ranging from spherical to elongated needles. Usually both morphologies are observed in the same sample.

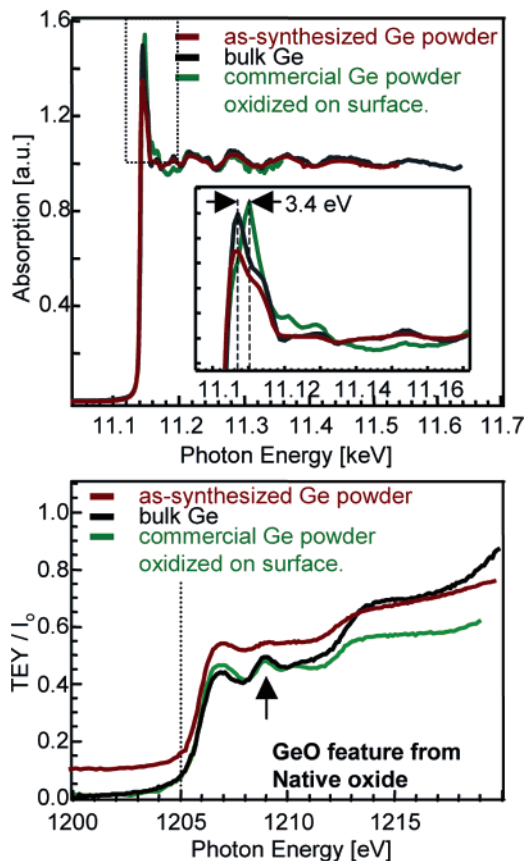


Figure 5. EXAFS (top) and XANES (bottom) spectra of the as-synthesized powder, bulk Ge, and a commercial surface-oxidized Ge powder. Spectra are measured at the K and L Ge edges, respectively. Notice how the EXAFS oscillation of the as-synthesized powder nicely matches the oscillation of bulk Ge. Also, XANES shows a native GeO feature in bulk Ge that is almost absent in as-synthesized Ge powders. The XANES spectrum of the as-synthesized Ge powder is offset for clarity. Measurements have been taken at the Advanced Light Source of the LBNL in Berkeley on beamline 10.3.2 (micro-EXAFS) and beamlines 8.0.1 and 11.02 (XANES).

Although we cannot exclude that these as-synthesized powders are polycrystalline Ge, a careful observation of such TEM images suggests that they are likely aggregates of smaller particles. This view is supported by HRTEM and electron diffraction analyses of these powders near their edges (when possible), which clearly reveal monocrystalline germanium of ~ 3 nm to ~ 10 nm embedded in a matrix (Figure 4). The size distribution of the Ge nanocrystals inside the as-synthesized powders is not known, but it may be different from the size distribution determined by TEM of a fraction of the powder dissolved in solvents. For every as-synthesized powder, qualitative energy-dispersive X-ray (EDX) analysis of such large aggregates indicates the presence of only Ge and C. X-ray absorption near edge structure (XANES) and extended X-ray absorption fine structure (EXAFS) spectra of the powders at the Ge L and K edges, respectively, (Figure 5) exhibit bulk-like behavior, as it was observed for pure Ge clusters larger than ~ 5 nm.⁸ The EXAFS oscillations are the same as those of bulk Ge, but differ markedly from those of commercial Ge powder whose surface is oxidized. Similarly, the absorption onset

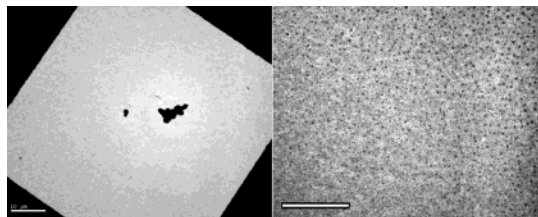


Figure 6. TEM images of a Ge powder subjected to heating at 600 °C in air for 12 h. In general, we still see large aggregates (left), but fields of isolated particles can be observed at higher magnification (right). These particles are shapeless and are <5 nm in diameter. Bars: 10 μ m (left); 100 nm (right).

and slope of the XANES spectra almost overlap. This shows evidence of tetrahedrally bonded germanium in the as-synthesized powder and indicates that the organogermane contribution is at most a tiny fraction of the dominant elemental Ge. Also, the spectra do not exhibit strong oxide features.

The lack of air sensitivity of the Ge powders is an indication of the presence of strong-binding surfactants that fully passivate the Ge surface. Given the results of EDX chemical profiling, we can speculate that the surface contains either Ge–H or Ge–C bonds. Unfortunately, XANES analysis cannot probe the surface composition of the Ge dots because the total electron yield measurements (TEY) at 1200 eV have a probe depth of \sim 50–100 nm.¹⁹ Therefore, the surface composition is largely unknown. One likely possibility is the presence of a Ge–C shell due to the decomposition of organic molecules at high temperatures. Such hydrocarbon coating is consistent with the spacing of 1–2 nm between nanoparticles revealed by TEM images of Ge nanocrystal assemblies (Figure 2G for instance) and may explain why we obtain nanocrystals and not bulk polycrystalline Ge, even if there are no surfactants in the initial solution.

Synchrotron studies and XRD and EDX data indicate that the matrix which embeds the Ge nanocrystals is amorphous and contains mostly hydrocarbons. Further carbon 1s NEXAFS spectroscopy using scanning transmission X-ray microscopy (STXM) indicates the presence of mainly C=C bonds ($1s \rightarrow \pi^*$ and $1s \rightarrow \sigma^*$ transitions), C–C ($1s \rightarrow \sigma^*$), and C–H ($1s \rightarrow \pi^*$ and $1s \rightarrow \sigma^*$) bonds, although the exact nature of the matrix is still unknown. Therefore, it is difficult to find a chemical method to fully dissolve the matrix in a consistent way so as to isolate the nanocrystals. We have investigated a wide variety of solvents from formic acid to nonanoic acid, and their alcohol counterparts with mixed results. We have also tried to burn the matrix in air at 600 °C. In this case the powder loses \sim 5% of its weight, and XRD analysis still exhibits an identical diffraction pattern. The suspension of the heated powder in toluene and subsequent TEM analysis reveals two features. First, the major part of the as-synthesized powder seems morphologically intact (Figure 6A). Second, a tiny fraction of Ge nanocrystals (\sim 4 nm) can be observed at higher magnification (Figure 6b). Such dissolution approaches are encouraging but do not free a significant fraction of nanocrystals yet.

Alternative dissolution approaches such as Ar, N₂, or H₂ plasma cleaning or carbon burnout shall be investigated.²⁰

The growth mechanism and limiting factors in the growth of the Ge nanocrystals are yet unclear. It is surprising that syntheses carried out on time scales ranging from 1 to 30 min yield nanoparticles with almost similar sizes. This suggests a fast nucleation process. However, once formed, the Ge nanoparticles may possess a robust coating on their surface which prevents further growth. We expect to gain more information on the growth mechanism at high temperatures by further in-depth studies of anisotropic Ge rods. We believe that Ge rods are not linear aggregates of nanoparticles, since we have observed (Figure 2I for instance) the simultaneous presence of elongated and spherical particles with clearly different sizes. An interesting question concerns the size and shape distribution of the Ge nanoparticles inside the matrix. When we succeed in dissolving this matrix and image the nanoparticles on a TEM grid, the size distribution of the particles, determined by counting and statistical analysis from TEM pictures, is rather homogeneous (see Supporting Information). Such analysis only probes the fraction of the particles observed on the grid. The presence inside the matrix of a fair amount of slightly larger or smaller crystals cannot be ruled out.

The large amount of residual byproducts in the powders prevents a thorough investigation of the optical properties of the Ge nanocrystals. As a matter of fact, C 1s NEXAFS spectroscopy shows the presence of C=C bonds in our samples, even when pure TEG is thermally decomposed. Furthermore, most pure organics we have tested show a strong blue fluorescence after being heated to >400 °C. These observations suggest that simple aliphatic chains decompose at high temperature and form conjugated unsaturated systems or simple alkene chains. The fluorescence of these byproducts could be mistakenly attributed to Ge nanocrystals. Therefore, conclusive assertions on optical properties of quantum dots, based on absorption and fluorescence measurements of solutions, are premature if the samples have not been thoroughly cleaned.

Our two-step synthesis has the potential to produce gram quantities of Ge nanocrystals. However, we see two difficulties associated with our approach. The first is the issue of size control; the second is related to the dissolution of the matrix. It may be possible to influence the size of the dots with a more elaborate design of the reactor. The design of an injection system into a hot vessel would be a first step toward such improvements. A second issue is the clustering of the Ge nanocrystals inside the matrix. Such clustering may be unavoidable at high temperatures because of the presence of organic free radicals due to the decomposition of the organogermane and/or the solvents. Therefore, we are investigating alternative methods to post-process the Ge powders and free the embedded nanocrystals. Work is in progress to answer some unresolved issues: (1) determine the real size distribution of the Ge nanocrystals; (2) understand why nanocrystals on a TEM grid self-assemble; (3) unravel the mechanism of formation of Ge nanocrystals and rods. Finally, the dissolution of the matrix and the

cleaning of the solution from any remaining byproduct will allow us to answer the long standing and still unresolved (in our opinion) issue of the optical properties of such Ge nanocrystals.

Acknowledgment. We thank Jennifer Harper for help with the HRTEM and David Prendergast for comments on the manuscript. S.F. thanks D. K. Shuh and M. A. Marcus for providing beamtime on ALS STXM at beamline 11.0.2 and Micro-Exafs beamline 10.3.2 respectively. TVB thanks the ALS for beamtime at beamline 8.0.1. Low resolution TEM measurements were performed at the Electron Microscope Lab of U.C. Berkeley, and we thank Reena Zalpuri for assistance. This work was performed under the auspices of the U.S. Department of Energy at the University of California/Lawrence Livermore National Laboratory under Contract No. W-7405-Eng-48. Beamlines 11.0.2 and 10.3.2 and 8.0.1 of the Advanced Light Source are supported by the Director, Office of Science, Office of Basic Energy Sciences, Division of Chemical Sciences, Geosciences, and Biosciences and the Division of Materials Sciences of the U.S. Dept of Energy at Lawrence Berkeley National Laboratory under Contract No. DE-AC03-76SF.00098.

Supporting Information Available: Additional TEM images from sample Ge₃ after nonanoic acid treatment. This material is available free of charge via the Internet at <http://pubs.acs.org>.

References

- (1) Kovalev, D.; Heckler, H.; Polisski, G.; Koch, F. *Phys. Status Solidi B* **1999**, *215*, 871–932.

- (2) She, M.; King, T. J. *IEEE Trans. Electron Dev.* **2003**, *50*, 1934–1940.
- (3) Bettotti, P.; Cazzanelli, M.; Dal Negro, L.; Danese, B.; Gaburro, Z.; Oton, C. J.; Prakash, G. V.; Pavesi, L. *J. Phys.: Condens. Matter* **2002**, *14*, 8253–8281.
- (4) Canham, L. T. *Appl. Phys. Lett.* **1990**, *57*, 1046–1048.
- (5) Iacona, F.; Franzo, G.; Spinella, C. *J. Appl. Phys.* **2000**, *87*, 1295–1303.
- (6) Qu, X. X.; Chen, K. J.; Huang, X. F.; Li, Z. F.; Feng, D. *Appl. Phys. Lett.* **1994**, *64*, 1656–1658.
- (7) Min, K. S.; Shcheglov, K. V.; Yang, C. M.; Atwater, H. A.; Brongersma, M. L.; Polman, A. *Appl. Phys. Lett.* **1996**, *68*, 2511–2513.
- (8) Bostedt, C.; van Buuren, T.; Plitzko, J. M.; Moller, T.; Terminello, L. J. *J. Phys.: Condens. Matter* **2003**, *15*, 1017–1028.
- (9) Wilcoxon, J. P.; Provencio, P. P.; Samara, G. A. *Phys. Rev. B* **2001**, *64*, 035417.
- (10) Wilcoxon, J. P.; Samara, G. A.; Provencio, P. N. *Phys. Rev. B* **1999**, *60*, 2704–2714.
- (11) Baldwin, R. K.; Pettigrew, K. A.; Ratai, E.; Augustine, M. P.; Kauzlarich, S. M. *Chem. Commun.* **2002**, 1822–1823.
- (12) Baldwin, R. K.; Pettigrew, K. A.; Garno, J. C.; Power, P. P.; Liu, G. Y.; Kauzlarich, S. M. *J. Am. Chem. Soc.* **2002**, *124*, 1150–1151.
- (13) Heath, J. R. *Science* **1992**, *258*, 1131–1133.
- (14) Holmes, J. D.; Ziegler, K. J.; Doty, R. C.; Pell, L. E.; Johnston, K. P.; Korgel, B. A. *J. Am. Chem. Soc.* **2001**, *123*, 3743–3748.
- (15) English, D. S.; Pell, L. E.; Yu, Z. H.; Barbara, P. F.; Korgel, B. A. *Nano Lett.* **2002**, *2*, 681–685.
- (16) Heath, J. R.; Shiang, J. J. *Chem. Soc. Rev.* **1998**, *27*, 65–71.
- (17) Green, M. *Curr. Opin. Solid State Mater. Sci.* **2002**, *6*, 355–363.
- (18) Geddes, R. L.; Mack, E. J. *J. Am. Chem. Soc.* **1930**, *52*, 4372–4380.
- (19) Erbil, A.; Cargill, G. S.; Frahm, R.; Boehme, R. F. *Phys. Rev. B* **1988**, *37*, 2450–2464.
- (20) El Boucham, J.; Maury, F.; Morancho, R. *J. Anal. Appl. Pyrol.* **1998**, *44*, 153–165.

NL035231T